Journal of Solid State Chemistry **142,** 279–287 (1999)
Article ID jssc.1998.8012, available online at http://www.idealibrary.com on IDEAL®

Quaternary Silicide Carbides AT_2SiC (A = Rare Earth Elements and Actinoids, T = Mn, Re, Ru, Os) with $DyFe_2SiC$-Type Structure

Thomas Hüfken, Anne M. Witte, and Wolfgang Jeitschko[1]

Anorganisch-Chemisches Institut, Universität Münster, Wilhelm-Klemm-Strasse 8, D-48149 Münster, Germany

Received March 5, 1998; in revised form August 20, 1998; accepted August 21, 1998

The 49 compounds AMn_2SiC (A = Y, Sm, Gd–Tm, Lu, Th, U), ARe_2SiC (A = Y, Ce–Nd, Sm, Gd–Tm, Th), ARu_2SiC (A = Y, Ce–Nd, Sm, Gd–Tm, Th), and AOs_2SiC (A = Y, La–Nd, Sm, Gd–Tm, Th, U) have been prepared for the first time. They crystallize with $DyFe_2SiC$-type structure, which was refined for $PrOs_2SiC$ from single-crystal X-ray data: *Cmcm*, $a = 396.02(5)$ pm, $b = 1105.8(1)$ pm, $c = 717.2(1)$ pm, $Z = 4$, $R = 0.030$ for 320 structure factors F and 18 variable parameters V. The refinement of the occupancy parameters revealed that the silicon site contains 2.0(3)% osmium. Mixed occupancy for this site resulted also from two structure refinements of the corresponding thorium compound, yielding the compositions $ThOs_{2.040(2)}Si_{0.960(2)}C$ ($a = 396.41(7)$ pm, $b = 1115.5(1)$ pm, $c = 717.0(1)$ pm, $R = 0.013$, 245 F, 18 V) and $ThOs_{2.284(2)}Si_{0.716(2)}C$ ($a = 397.1(1)$ pm, $b = 1113.9(2)$ pm, $c = 724.5(1)$ pm, $R = 0.025$, 483 F, 18 V). No such deviations from the ideal compositions were detected by the (less accurate) Rietveld refinements of the structures of $TbRe_2SiC$, $DyRu_2SiC$, and $HoRu_2SiC$. Magnetic susceptibility measurements with a SQUID magnetometer indicate Pauli paramagnetism for YRu_2SiC and YOs_2SiC. Chemical bonding in the $DyFe_2SiC$-type compounds is discussed. It is shown that an electron count of 18 can be achieved for most of the transition metal atoms.

INTRODUCTION

While searching for new permanent magnets Paccard, Paccard, and Bertrand prepared the compound $DyFe_2SiC$ and reported its crystal structure, which was of a new type (1). More recently, we characterized the corresponding compounds AFe_2SiC (A = Y, Sm, Gd, Tb, Ho–Tm, Lu, Th, U) and refined the structure of $ThFe_2SiC$ (2). We have explored the stability range of this quaternary structure type and now report on isotypic silicide carbides with manganese, rhenium, ruthenium, and osmium as transition metal components. A preliminary account of this work has been presented at a conference (3).

[1] To whom correspondence should be addressed.

SAMPLE PREPARATION, PROPERTIES, AND LATTICE CONSTANTS

Starting materials were ingots of the rare earth metals and thorium, platelets of uranium (Merck, "nuklearrein"), powders of the transition metals (all with nominal purities $> 99.9\%$), and graphite flakes (Alfa, $> 99.5\%$). Filings of the rare earth elements and thorium were prepared under dried (Na) paraffin oil. The oil was removed with *n*-hexane. Because of their reactivity, the filings of yttrium, the early lanthanoids, and thorium had to be stored under vacuum. The uranium platelets were cleaned with concentrated nitric acid to remove oxide impurities.

The samples with ruthenium and osmium as transition metal components were prepared by arc-melting small (about 400 mg) cold-pressed pellets of the elements with the ideal atomic ratio in an atmosphere of purified argon. The samples were melted from both sides to enhance their homogeneity. The compounds $LaOs_2SiC$ and $PrOs_2SiC$ could not be synthesized by this technique. They were obtained from samples which were sealed in silica tubes. These samples were then melted in a high-frequency furnace and immediately thereafter the temperature was lowered below the melting point. At that temperature the samples were annealed for 8 h, followed by rapid cooling. The outsides of the silica tubes were cooled by flowing water to prevent their reaction with the hot samples.

For the arc-melting of the samples containing manganese, an excess of manganese had to be used because of its low boiling point. Attempts with the composition 1:4:1:1 were usually successful.

The quaternary compounds with rhenium as the transition metal component were prepared in two steps. Equiatomic ternary alloys of the three components A, rhenium, and silicon were reacted by arc-melting cold-pressed pellets. Then the resulting ingots were ground to powder and cold-pressed together with stoichiometric amounts of graphite. The resulting pellets were again arc-melted at least twice. The phases could not be synthesized by the reaction of all four components in the arc-melting furnace, because

0022-4596/99 $30.00

these reactions are too violent, resulting in the partial loss of the samples.

The quaternary silicide carbides AT_2SiC, with the exceptions of LaO_2SiC and $PrOs_2SiC$ (see above), were present in the arc-melted ingots, but nevertheless, the samples were wrapped in tantalum foil and annealed in evacuated silica tubes for 1 month at 1000°C to enhance their homogeneity.

The new compounds are all stable in air for long periods of time. Well-crystallized samples have a light gray color with metallic luster; the powders are dark gray. Energy dispersive X-ray fluorescence analyses (EDX) of the silicide carbides in a scanning electron microscope did not reveal any impurity elements heavier than sodium (detectability limit 2 at.%).

Guinier powder diagrams of the samples were recorded with Cu$K\alpha_1$ radiation and α-quartz ($a = 491.30$ pm, $c = 540.46$ pm) as an internal standard. The identification of the diffraction lines was facilitated by intensity calculations (4) using the positional parameters of the refined structures of $TbRe_2SiC$, $DyRu_2SiC$, $HoRu_2SiC$, $PrOs_2SiC$, and $ThOs_2SiC$, respectively. The lattice constants, obtained by least-squares fits, are listed in Table 1. The cell volumes (Fig. 1) reflect the lanthanoid contraction.

TABLE 1
Lattice Constants of Carbides with the Orthorhombic $DyFe_2SiC$ Type Structure[a]

Compound	a (pm)	b (pm)	c (pm)	V (nm^3)
YMn_2SiC	370.4(1)	1066.0(2)	703.8(1)	0.2779
$SmMn_2SiC$	379.0(1)	1073.3(3)	708.6(1)	0.2882
$GdMn_2SiC$	375.5(1)	1069.1(1)	706.8(1)	0.2837
$TbMn_2SiC$	372.6(1)	1066.4(2)	704.9(1)	0.2801
$DyMn_2SiC$	370.2(1)	1063.3(1)	703.2(1)	0.2768
$HoMn_2SiC$	368.5(1)	1063.3(1)	703.1(1)	0.2755
$ErMn_2SiC$	366.8(1)	1063.0(2)	702.1(1)	0.2738
$TmMn_2SiC$	364.1(1)	1062.4(2)	700.3(1)	0.2709
$LuMn_2SiC$	360.9(1)	1063.2(2)	698.2(1)	0.2679
$ThMn_2SiC$	383.2(1)	1092.1(1)	715.2(1)	0.2993
UMn_2SiC	365.61(6)	1076.5(2)	699.8(1)	0.2754
YRe_2SiC	394.45(5)	1089.6(1)	722.0(1)	0.3103
$CeRe_2SiC$	404.36(4)	1094.0(1)	727.68(9)	0.3219
$PrRe_2SiC$	404.08(6)	1093.7(1)	727.8(1)	0.3216
$NdRe_2SiC$	402.70(4)	1092.2(1)	727.28(9)	0.3199
$SmRe_2SiC$	400.03(6)	1091.0(1)	725.3(1)	0.3165
$GdRe_2SiC$	397.67(5)	1088.9(1)	723.7(1)	0.3134
$TbRe_2SiC$	395.71(7)	1088.8(2)	723.0(2)	0.3115
$DyRe_2SiC$	393.93(5)	1087.4(1)	721.8(1)	0.3092
$HoRe_2SiC$	393.09(4)	1088.59(7)	721.48(6)	0.3087
$ErRe_2SiC$	391.47(5)	1088.3(1)	720.8(1)	0.3071
$TmRe_2SiC$	390.36(5)	1087.4(1)	720.3(1)	0.3058
$ThRe_2SiC$	399.83(6)	1112.4(2)	735.4(1)	0.3271
YRu_2SiC	377.5(1)	1107.1(1)	713.3(1)	0.2981
$CeRu_2SiC$	390.3(1)	1108.1(1)	715.7(1)	0.3095
$PrRu_2SiC$	391.4(1)	1106.8(1)	719.3(1)	0.3116
$NdRu_2SiC$	388.9(1)	1106.0(1)	719.5(1)	0.3095
$SmRu_2SiC$	384.7(1)	1105.0(1)	717.0(1)	0.3048
$GdRu_2SiC$	382.1(1)	1105.5(1)	714.5(1)	0.3018
$TbRu_2SiC$	379.6(1)	1105.6(2)	714.2(1)	0.2997
$DyRu_2SiC$	376.7(1)	1105.3(3)	713.8(2)	0.2972
$HoRu_2SiC$	375.6(1)	1106.6(1)	712.9(1)	0.2963
$ErRu_2SiC$	374.2(1)	1107.4(2)	711.0(1)	0.2946
$TmRu_2SiC$	372.0(1)	1109.6(2)	710.8(1)	0.2934
$ThRu_2SiC$	392.1(1)	1115.3(2)	718.0(2)	0.3140
YOs_2SiC	384.50(4)	1105.5(1)	711.2(1)	0.3023
$LaOs_2SiC$	400.3(3)	1108.9(2)	719.9(1)	0.3195
$CeOs_2SiC$	395.10(4)	1106.4(1)	714.4(1)	0.3123
$PrOs_2SiC$	396.02(5)	1105.8(1)	717.2(1)	0.3141
$NdOs_2SiC$	394.00(5)	1105.0(1)	717.24(7)	0.3123
$SmOs_2SiC$	390.68(5)	1104.0(1)	714.2(1)	0.3080
$GdOs_2SiC$	388.48(6)	1103.9(1)	713.7(1)	0.3061
$TbOs_2SiC$	386.41(6)	1104.4(1)	712.8(1)	0.3042
$DyOs_2SiC$	384.41(6)	1104.3(2)	711.3(2)	0.3020
$HoOs_2SiC$	383.22(3)	1104.57(7)	709.10(7)	0.3002
$ErOs_2SiC$	381.99(5)	1105.6(1)	708.98(9)	0.2994
$TmOs_2SiC$	380.19(6)	1106.4(1)	707.47(8)	0.2976
$ThOs_2SiC$	396.41(7)	1115.5(1)	717.0(1)	0.3171
UOs_2SiC	385.79(7)	1116.6(2)	701.1(1)	0.3020

[a] Standard deviations in the positions of the least significant digits are given in parentheses throughout this paper.

MAGNETIC SUSCEPTIBILITIES OF YRu_2SiC AND YOs_2SiC

Susceptibility measurements of YRu_2SiC and YOs_2SiC were carried out in the temperature range between 2 and 300 K with a SQUID magnetometer (SHE Quantum Design, Inc.) with magnetic flux densities of up to 5.5 T. The samples were cooled in zero field and the susceptibilities were recorded continuously on heating. The susceptibilities are very small, not field-dependent, and nearly temperature-independent at temperatures above 150 K (Fig. 2). These characteristics are typical of Pauli paramagnetism. The upturns of the susceptibilities at low temperatures may be ascribed to paramagnetic impurities and paramagnetic surface states of the powder samples. Nevertheless, we have evaluated these data according to the modified Curie–Weiss law $\chi = \chi_0 + C/(T - \Theta)$, and we obtained for the temperature-independent parts the values $\chi_0 = 1.7(\pm 0.1) \times 10^{-9}$ m^3 per formula unit (f.u.) for YRu_2SiC and $\chi_0 = 2.6(\pm 0.2) \times 10^{-9}$ m^3/f.u. for YOs_2SiC. The temperature-dependent parts of the susceptibilities were evaluated with the equation $\mu_{exp} = 2.83\ [\chi(T - \Theta)]^{1/2}$. This resulted in the magnetic moments of $\mu_{exp} = 0.48\ \mu_B$ and $\mu_{exp} = 0.35\ \mu_B$ for the samples of YRu_2SiC and YOs_2SiC, respectively. These values are much smaller than the value of $\mu_{eff} = 1.73\ \mu_B$/f.u. expected for one d-electron with an uncompensated spin.

STRUCTURE REFINEMENTS

Single crystals of $PrOs_2SiC$ and $ThOs_2SiC$ were isolated from crushed samples prepared in the high-frequency furnace as described above. They were investigated with a Buerger precession camera to establish their suitability for the intensity data collection. These data were measured using an Enraf Nonius CAD4 diffractometer with

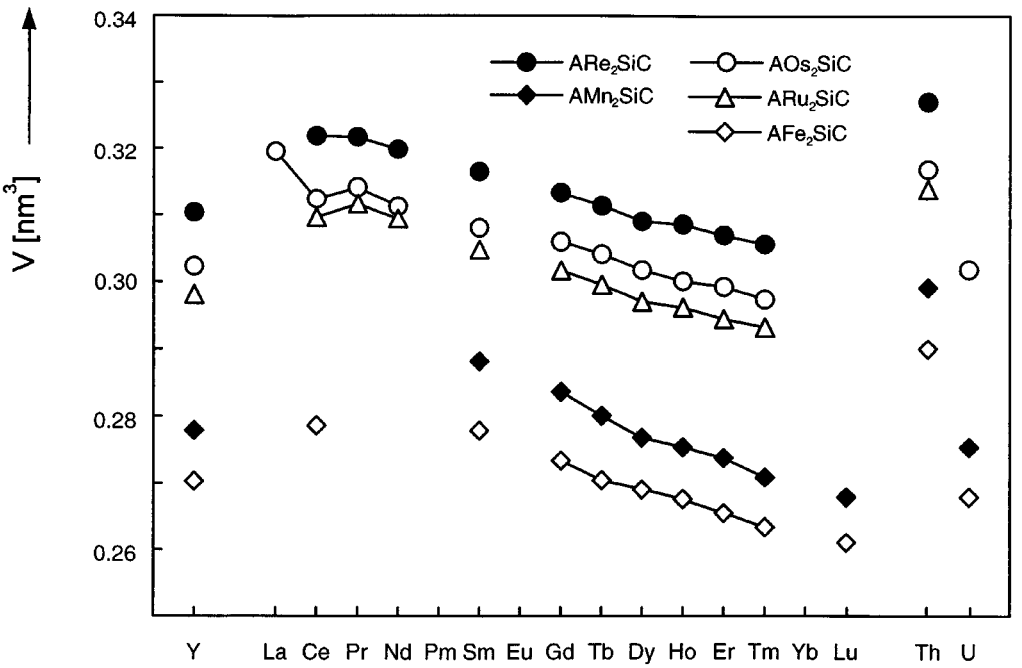

FIG. 1. Cell volumes of $DyFe_2SiC$-type carbides. The data for the iron-containing compounds were taken from Ref. (2).

graphite-monochromated Mo$K\alpha$ radiation and a scintillation counter with pulse-height discrimination. The crystallographic data and some details of the structure refinements are summarized in Table 2. The values of the lattice constants found for $PrOs_2SiC$ and for the first crystal of $ThOs_2SiC$, using the four-circle diffractometer, are in good agreement with the lattice constants obtained from the Guinier powder data. A second crystal of $ThOs_2SiC$ was isolated from an inhomogenous sample, which also had been prepared in the high-frequency furnace. The c parameter of this latter crystal, as determined on the four-circle diffractometer, was considerably larger than the one refined from the Guinier powder data. This suggested that this crystal had a different composition than most of the sample, a fact confirmed by the structure determination. This crystal was again analyzed after the data collection, and the EDX analysis did not reveal any heavy elements besides thorium, osmium, and silicon.

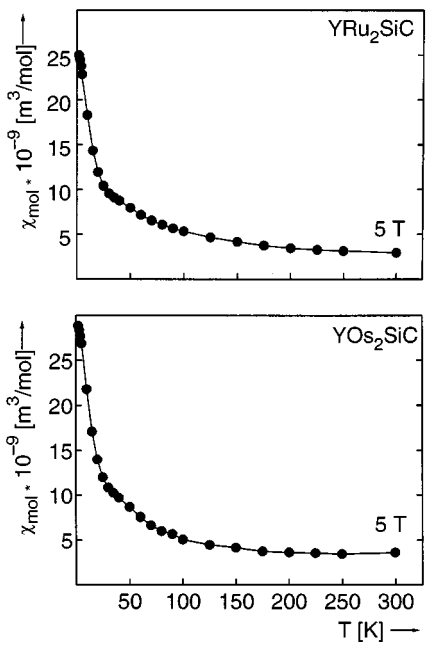

FIG. 2. Magnetic susceptibilities of YRu_2SiC and YOs_2SiC as a function of temperature.

Starting with the positional parameters of $ThFe_2SiC$, the structures were refined by a full-matrix least-squares program (5), with atomic scattering factors, corrected for anomalous dispersion as provided for by that program. The weighting schemes were based on the counting statistics, and a parameter correcting for isotropic secondary extinction was optimized during each refinement. The metal and silicon atoms were refined with anisotropic displacement parameters and the carbon atoms with isotropic displacement parameters. However, in all structure refinements from single-crystal data, the displacement parameters of the silicon atoms were abnormally low, indicating an admixture of some heavier element on the silicon site. It is well known that the late transition elements can substitute for the silicon atoms in silicides with a high metal content (6). The only other heavy components of the compounds are the rare

TABLE 2
Crystallographic Data for $PrOs_{2.020}Si_{0.980}C$, $ThOs_{2.040}Si_{0.960}C$, and $ThOs_{2.284}Si_{0.716}C$

Compound	$PrOs_{2.020}Si_{0.980}C$	$ThOs_{2.040}Si_{0.960}C$ crystal 1	$ThOs_{2.284}Si_{0.716}C$ crystal 2
Lattice constants (pm)	$a = 395.8(1)$	$a = 396.60(4)$	$a = 397.1(1)$
(single crystal diffractometer)	$b = 1105.5(2)$	$b = 1115.9(3)$	$b = 1113.9(2)$
	$c = 716.6(1)$	$c = 716.6(1)$	$c = 724.5(1)$
Space group	*Cmcm* (No. 63)	*Cmcm* (No. 63)	*Cmcm* (No. 63)
Formula units/cell (Z)	4	4	4
Formula mass	564.65	659.02	698.58
Calculated density (g/cm^3)	11.93	13.80	14.48
Crystal dimensions (μm^3)	$30 \times 30 \times 80$	$25 \times 25 \times 90$	$30 \times 30 \times 80$
$\theta/2\theta$ scans up to	$2\theta = 70^\circ$	$2\theta = 90^\circ$	$2\theta = 85^\circ$
Range in h, k, l	± 6, ± 17, ± 11	± 7, ± 22, ± 14	± 7, ± 20, $0 - 13$
Total no. of reflections	2744	5233	2411
Absorption correction from psi scans			
Transmission (highest/lowest)	1.12	1.23	1.72
Unique reflections	426	780	687
Merging residual (R_i)	0.029	0.033	0.037
Reflections with $I > 3\sigma(I_o)$	320	245	483
No. of variables	18	18	18
Highest residual electron density (e/Å^3)	1.9	0.7	2.2
Conventional residual (R on F values)	0.030	0.013	0.025
Weighted residual (R_w)	0.033	0.015	0.026

earth and thorium atoms. As these are certainly too large to substitute for the silicon atoms, we refined this site with mixed silicon/osmium occupancy. These refinements resulted in a Si/Os2 occupancy of 0.980(3)/0.020 for $PrOs_2SiC$, 0.960(2)/0.040 for crystal *1*, and 0.716(2)/0.284 for crystal *2* of $ThOs_2SiC$. These occupancy values correspond to the exact compositions $PrOs_{2.020}Si_{0.980}C$, $ThOs_{2.040}Si_{0.960}C$, and $ThOs_{2.284}Si_{0.716}C$. No significant deviations from full occupancy were found for the other atomic positions, nor was there any evidence for the occupancy of additional atomic sites from the final difference Fourier syntheses. The highest residual electron densities had small values (Table 2), and they were all at locations too close to the metal

TABLE 3
Atomic Parameters of $PrOs_{2.020(3)}Si_{0.980(3)}C$, $ThOs_{2.040(2)}Si_{0.960(2)}C$, and $ThOs_{2.284(2)}Si_{0.716(2)}C$ Refined from Single-Crystal Data[a]

Atom	*Cmcm*	Occupancy	x	y	z	B
$PrOs_{2.020(3)}Si_{0.980(3)}C$						
Pr	4*c*	0.994(4)	0	0.0486(1)	1/4	0.45(2)
Os1	8*f*	1.003(2)	0	0.66712(5)	0.55931(8)	0.350(7)
Si/Os2	4*c*	0.980(3)/0.020	0	0.7698(5)	1/4	0.43(8)
C	4*b*	0.91(5)	0	1/2	0	0.5(3)
$ThOs_{2.040(2)}Si_{0.960(2)}C$						
Th	4*c*	1.002(1)	0	0.05220(4)	1/4	0.335(6)
Os1	8*f*	0.998(1)	0	0.66608(2)	0.55632(5)	0.316(5)
Si/Os2	4*c*	0.960(2)/0.040	0	0.7731(2)	1/4	0.38(4)
C	4*b*	0.94(3)	0	1/2	0	0.4(2)
$ThOs_{2.284(2)}Si_{0.716(2)}C$						
Th	4*c*	1.002(1)	0	0.04877(5)	1/4	0.335(6)
Os1	8*f*	0.998(1)	0	0.66686(3)	0.55538(5)	0.351(4)
Si/Os2	4*c*	0.716(2)/0.284	0	0.7735(1)	1/4	0.36(2)
C	4*b*	0.91(4)	0	1/2	0	0.4(1)

[a] The last column contains the isotropic displacement parameters of the carbon atoms and the equivalent isotropic displacement parameters ($\times 10^4$, in units of pm^2) of the metal and silicon atoms. The occupancy parameters were refined in separate least-squares cycles. In the final cycles the ideal occupancies were assumed except for the Si/Os2 position.

TABLE 4
Crystallographic Data for $TbRe_2SiC$, $DyRu_2SiC$, and $HoRu_2SiC$

Compound	$TbRe_2SiC$	$DyRu_2SiC$	$HoRu_2SiC$
Lattice constants (pm)	$a = 396.482(8)$	$a = 377.657(9)$	$a = 376.273(9)$
(powder diffractometer)	$b = 1089.44(2)$	$b = 1107.03(3)$	$b = 1108.32(3)$
	$c = 722.85(1)$	$c = 714.99(2)$	$c = 714.08(2)$
Formula mass	571.42	404.74	407.17
Calculated density (g/cm^3)	12.18	9.05	9.13
Range in 2θ (°)	10–100	20–90	20–90
Step width in 2θ (°)	0.02	0.02	0.02
Total measuring time (h)	66	42	48
Total number of steps	4500	3501	3501
Number of reflections (LnT_2SiC)	104	84	84
Total no. of parameters	24	15	15
No. of structural parameters	7	6	6
Goodness of fit (χ^2)	8.42	5.46	11.1
Bragg residual (R_{Br})	0.035	0.034	0.032
Conventional residual (R_F)	0.035	0.030	0.031

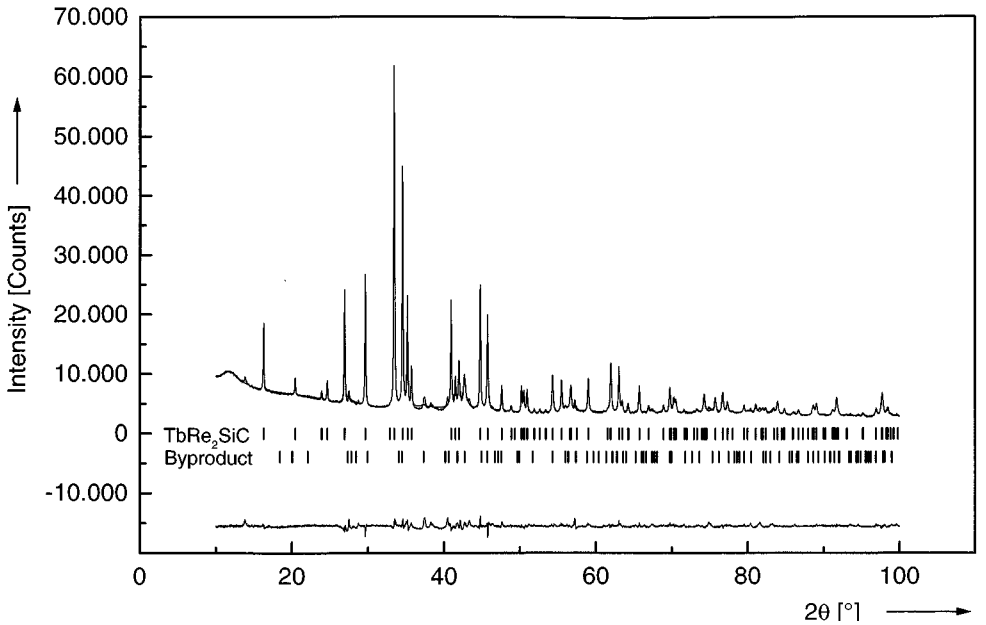

FIG. 3. Rietveld refinement plot for $TbRe_2SiC$. In the uppermost part of the plot the measured intensity values are indicated by dots and the calculated fit (superimposed) by a line. The peak positions of $TbRe_2SiC$ and the unknown tetragonal byproduct are indicated. The difference profile between the calculated and the observed plot is also shown.

positions to be suited for additional atomic sites. Hence, they could be ascribed to the insufficient correction for absorption, using the psi-scan method. The results of the single-crystal structure determinations are summarized in the Tables 2 and 3. The structure factor tables and the anisotropic thermal parameters of the single-crystal refinements are available from the authors (7, 8).

TABLE 5
Atomic Parameters of $TbRe_2SiC$, $DyRu_2SiC$, and $HoRu_2SiC$ Refined by the Rietveld Method[a]

Atom	*Cmcm*	*x*	*y*	*z*	*B*
$TbRe_2SiC$					
Tb	4*c*	0	0.0422(2)	1/4	0.68(5)
Re	8*f*	0	0.67309(9)	0.5621(1)	0.36(3)
Si	4*c*	0	0.7661(7)	1/4	0.5(2)
C	4*b*	0	1/2	0	0.8[b]
$DyRu_2SiC$					
Dy	4*c*	0	0.0462(1)	1/4	1.13(5)
Ru	8*f*	0	0.6636(1)	0.5561(2)	1.11(4)
Si	4*c*	0	0.7705(5)	1/4	0.5[b]
C	4*b*	0	1/2	0	0.5[b]
$HoRu_2SiC$					
Ho	4*c*	0	0.0456(1)	1/4	1.69(4)
Ru	8*f*	0	0.6640(1)	0.5566(2)	0.64(3)
Si	4*c*	0	0.7667(5)	1/4	0.5[b]
C	4*b*	0	1/2	0	0.5[b]

[a] The last column contains the isotropic displacement parameters ($\times 10^4$, in units of pm^2).

[b] These values were not refined.

The crystal structures of $TbRe_2SiC$, $DyRu_2SiC$, and $HoRu_2SiC$ were refined from X-ray powder diffractometer data by the Rietveld method using the FULLPROF program (9). The samples were ground to fine powders and placed on acetate foils. The X-ray intensity data were recorded from rotating samples on a focusing powder diffractometer (STOE Stadi P) with monochromated Cu$K\alpha_1$ radiation using a linear, position-sensitive detector in transmission geometry. Further details of these data collections and the structure refinements are summarized in Table 4. As an example, we show the Rietveld refinement plot for $TbRe_2SiC$ in Fig. 3.

All diffractograms revealed the existence of small amounts of other phases. For a second phase of the $TbRe_2SiC$ sample, indices were assigned using Visser's program (10) on the basis of a tetragonal cell with the lattice constants $a = 443.9(1)$ pm and $c = 963.7(1)$ pm. For $DyRu_2SiC$ and $HoRu_2SiC$ a few weak diffraction lines from unknown impurity phases (between 41.8 and 45.7° 2θ) were excluded from the refinements. In the final refinements of $TbRe_2SiC$, a total of 24 parameters were optimized, including the zero point, the scale factor, the lattice constants for $TbRe_2SiC$ and the tetragonal impurity phase, two asymmetry parameters, and for each phase four parameters to fit the peak profiles with pseudo-Voigt functions. The number of reflections attributable to $TbRe_2SiC$ was 104. In addition, 111 reflections of the impurity phase were fitted.

TABLE 6
Interatomic Distances in the Silicide Carbides AT_2SiC with $DyFe_2SiC$-Type Structure[a]

	$PrOs_{2.020}Si_{0.980}C$ single-crystal	$ThOs_{2.040}Si_{0.960}C$ single-crystal 1	$ThOs_{2.284}Si_{0.7160}C$ single-crystal 2	$TbRe_2SiC$ powder	$DyRu_2SiC$ powder	$HoRu_2SiC$ powder
A						
4 C	272.5	273.5	274.2	271.9(1)	264.4(1)	263.8(1)
1 Si	308.3	311.4	306.7	300.6(8)	304.8(6)	308.6(5)
2 Si	314.7	316.2	319.5	314.0(6)	311.3(5)	308.5(4)
4 *T*	325.0	322.0	325.1	332.2(1)	316.3(1)	316.5(1)
4 *T*	338.8	343.3	342.1	335.5(2)	329.2(2)	328.7(1)
2 *T*	342.8	343.6	346.7	338.4(2)	349.3(2)	349.7(2)
2 *A*	374.4	376.9	378.2	373.0(1)	371.3(1)	370.5(1)
2 *A*	396.0	396.4	397.1	395.7(1)	376.3(1)	375.6(1)
T						
1 C	189.6	189.6	190.2	193.7(1)	185.2(2)	185.9(1)
1 Si	249.2	250.0	251.1	247.3(3)	248.5(2)	246.4(3)
2 Si	250.6	251.3	252.4	249.0(2)	244.8(2)	245.3(2)
1 *T*	273.5	277.7	282.0	271.7(2)	276.8(2)	275.8(2)
2 *T*	282.9	284.4	283.1	274.3(1)	280.0(2)	279.4(1)
2 *A*	325.0	322.0	325.1	332.2(1)	316.3(1)	316.5(1)
2 *A*	338.8	343.3	342.1	335.5(2)	329.2(2)	328.7(1)
1 *A*	342.8	343.6	346.7	338.4(2)	349.3(2)	349.7(2)
Si						
2 *T*	249.2	250.0	251.1	247.3(3)	248.5(3)	246.4(3)
4 *T*	250.6	251.3	252.4	249.0(2)	244.8(2)	245.3(2)
1 *A*	308.3	311.4	306.7	300.6(8)	304.8(6)	308.6(5)
2 *A*	314.7	316.2	319.5	314.0(6)	311.3(5)	308.5(4)
C						
2 *T*	189.6	189.6	190.2	193.7(1)	185.2(2)	185.9(1)
4 *A*	272.5	273.5	274.2	271.9(1)	264.4(1)	263.8(1)

[a] All distances were computed with the lattice constants obtained from the Guinier powder data (Table 1) with the exception of $ThOs_{2.284}Si_{0.716}C$ (crystal 2), where the ones determined on the single crystal diffractometer (Table 2) were used. All distances shorter than 400 pm (*A*–*A*, *A*–*T*, *A*–Si, *A*–C) and 340 pm (all other distances) are listed. The standard deviations from the single crystal refinements are all 0.1 pm or less.

The intensities of the reflections of the carbide $TbRe_2SiC$ amounted for 85.7% of the scattering power of the total sample. For $DyRu_2SiC$ and $HoRu_2SiC$ only 15 parameters had to be fitted. The positional parameters and the isotropic displacement parameters of the metal atoms were refined independently, while the displacement parameters of the silicon and carbon atoms were held constant (Table 5). The interatomic distances of all structures are listed in Table 6, and a projection of the structure and the coordination polyhedra with $PrOs_2SiC$ as an example is shown in Fig. 4.

DISCUSSION

Twelve iron-containing $DyFe_2SiC$ type compounds have been known for some time (1, 2). With the presently reported manganese, rhenium, ruthenium, and osmium compounds this number has increased to 61.

The cell volumes of $CeRe_2SiC$, $CeFe_2SiC$, $CeRu_2SiC$, and $CeOs_2SiC$ deviate from the smooth functions interpolated or extrapolated from the volumes of the corresponding trivalent rare earth compounds. Hence, we expect cerium to be at least partially tetravalent in these silicide carbides. We have tried to prepare the corresponding ytterbium compounds by the same preparation technique (arc-melting of the components followed by annealing at lower temperatures), but, possibly because of the high vapor pressure of ytterbium, these compounds were not obtained. It may be possible to prepare these compounds by a different preparation technique, e.g., from a lithium flux. Since europium is even more volatile than ytterbium, we have not tried to prepare the corresponding europium compounds. In addition, it is well known that europium, because of its preference for the divalent state, frequently forms compounds with different structure types. The lutetium compounds with rhenium, ruthenium, and osmium were not obtained, possibly because lutetium is too small; similarly, the iron and manganese compounds with the early lanthanoids could up to now not be prepared, probably because these lanthanoids are too large to fit into the iron and manganese silicide carbide frameworks.

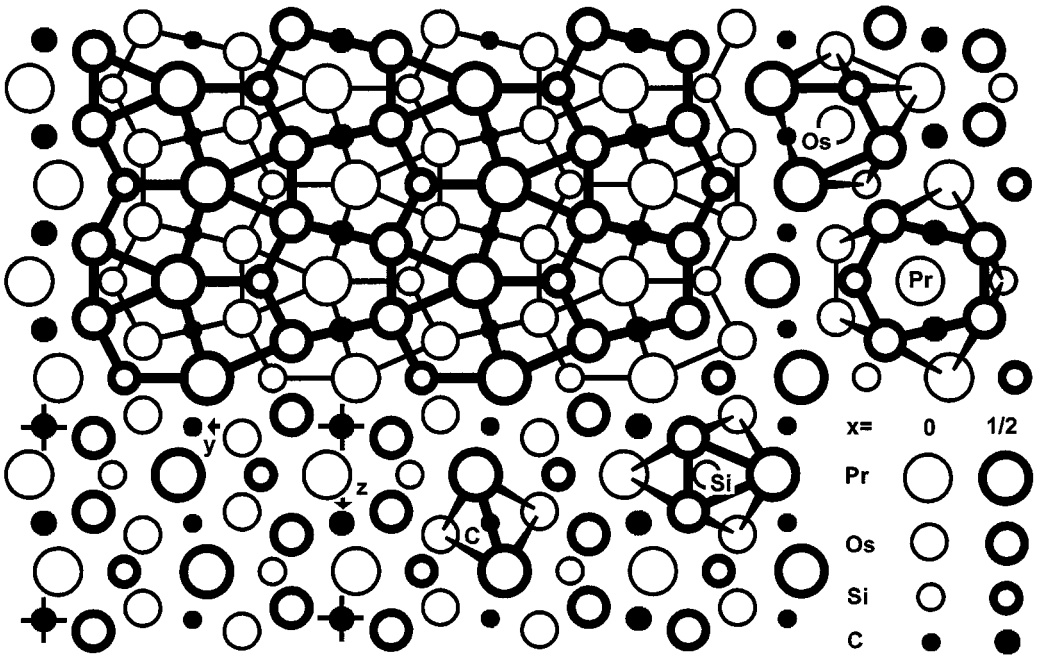

FIG. 4. Crystal structure and coordination polyhedra of $PrOs_2SiC$. Atoms connected by thick and thin lines in the lower left-hand part of the drawing are at $x = \frac{1}{2}$ and $x = 0$, respectively. These lines do not necessarily represent strong bonds.

Various aspects of the $DyFe_2SiC$ type structure have been discussed earlier (1, 2). In particular, it has been pointed out that it may be regarded as a filled-up (stuffed) Re_3B-type structure. Several ternary compounds may also be thought to crystallize with a filled Re_3B-type structure, e.g., V_3AsC (11, 12), Cr_3GeC (13), Zr_3AlN (14), and $UScS_3$ (15). However, it has been emphasized (2), that the carbon atoms in $DyFe_2SiC$ and $ThFe_2SiC$ occupy positions in these quaternary silicide carbides, which are different from the ones in the just-enumerated ternary compounds. The present structure refinements of $PrOs_2SiC$ and $ThOs_2SiC$ from single-crystal data clearly show that these two compounds are completely isostructural with $DyFe_2SiC$ and $ThFe_2SiC$, and this may also be assumed (with less certainty) for the other compounds reported here. This assumption is especially well-founded for $TbRe_2SiC$, for which the structure of the alternative model with carbon atoms at the position (0 0 0) rather than (0 1/2 0) was also refined. It was not possible to obtain a better fit with this alternative model, and the residuals were always higher by about 0.5% or more than those for the correct model.

The rare earth and thorium atoms are the most electropositive components of the $DyFe_2SiC$-type compounds, and for that reason we assume that most of their valence electrons are involved in bonding with the more electronegative carbon and silicon atoms, and to some extend also to the transition metal atoms. Hence, the carbon and silicon atoms together with the transition metal atoms may be considered to form a polyanion. This polyanion is emphasized in Fig. 5, with $PrOs_2SiC$ as an example. It consists of zig-zag chains of transition metal atoms, which extend along the x direction. These chains are linked by silicon atoms to form a puckered hexagonal close-packed sheet of composition Os_2Si (bottom of Fig. 5). In the third dimension, the osmium atoms of adjacent sheets are connected *via* carbon atoms in a linear Os–C–Os arrangement. The praseodymium atoms fill the remaining space between the sheets.

The compounds do not contain any silicon–silicon, silicon–carbon, or carbon–carbon bonds. Hence, silicon and carbon attain the oxidation number[2] -4, assuming that their s and p orbitals are fully involved in bonding with the A and transition metal components, i.e., assuming that they obey the octet rule. On the other hand, the A atoms form the most electropositive components of the compounds and therefore we count their valence electrons at the polyanion, neglecting any A–A bonding, an assumption, which may not be entirely justified (16). The important result of this counting procedure is that the osmium atoms in $PrOs_2SiC$ attain the oxidation number $+2.5$, corresponding to the formula $Pr^{+3}(Os^{+2.5})_2Si^{-4}C^{-4}$; i.e., the osmium atoms retain 5.5 valence electrons (a "$d^{5.5}$ system"), which are not involved in bonding with the other elements of the compound. These electrons may, however, form osmium–osmium bonds, thus

[2] Oxidation numbers are formal charges, where bonding electrons are *counted* at the atoms with the higher electronegativity, regardless of the partially covalent character of these bonds.

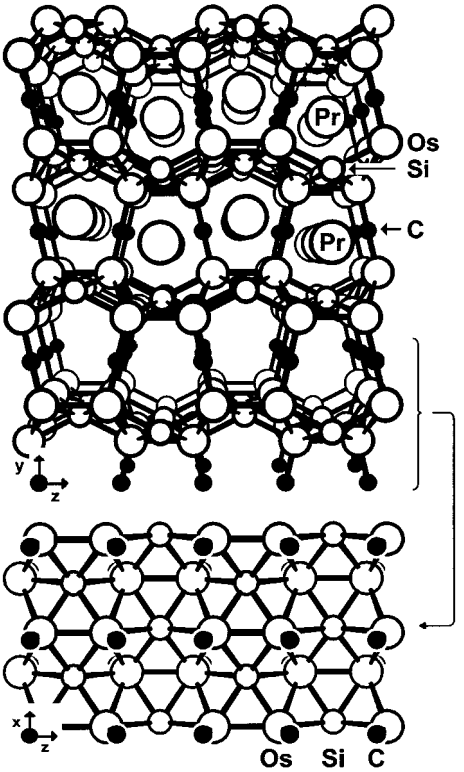

FIG. 5. The three-dimensionally infinite osmium–silicon–carbon network in the structure of PrO_2SiC. (Top) The whole structure is shown in a projection approximately along the *x* direction. (Bottom) The praseodymium atoms are omitted for clarity. It can be seen that there are two-dimensionally infinite osmium–silicon sheets, which are connected in the third dimension via carbon atoms. Such a sheet with the adjacent carbon atoms is shown in a view approximately along the *y* direction.

possibly increasing the electron count of the osmium atoms to 18 ("18-electron rule").

This is demonstrated in Table 7 for all atoms of one formula unit for three $DyFe_2SiC$-type compounds with different overall electron counts. The carbon atoms in $PrOs_2SiC$ form two bonds to the two neighboring osmium atoms (Os–C bond length: 189.6 pm, Table 6). In aiming for integer numbers (a restriction which is not required for a band structure), we may count two or four electrons for each of these interactions, corresponding to single or double bonds (case **A** or case **B** in the left-hand or right-hand side, respectively, for $PrOs_2SiC$ of Table 7). In the first case, the carbon atoms obtain two "lone pairs." These electrons may be involved in more or less covalent bonding toward the praseodymium atoms. In the second case, the carbon atoms have already used all of their valence orbitals to form the two double bonds to the osmium neighbors and no covalent praseodymium–carbon interactions are possible.

The silicon atoms have six osmium neighbors (at 249.2 pm (2 ×) and 250.6 pm (4 ×), respectively). For simplicity we count the eight valence electrons of the *s* and *p* orbitals of the silicon atoms as involved in silicon-osmium bonding, thus disregarding covalent praseodymium–silicon interactions. Hence, these electrons are also counted at the osmium atoms. Similarly, the electron count of the osmium atoms also contains the electrons of the carbon–osmium bonds. Finally, we have to count the 5.5 electrons per osmium atom, which are not involved in bonding toward the other elements. If we assume that they form Os–Os bonds, we have to count them at both of the bonded osmium atoms, and therefore we obtain 11 electrons per osmium atom for the Os–Os bonds. Thus, each osmium atom attains a total electron count of 17 (left-hand side of Table 7) or 19 (right-hand side of Table 7). The real situation will probably be in between these two extremes, since these compounds do not seem to contain localized electrons with uncompensated spins as is indicated by the Pauli paramagnetism of YRu_2SiC and YOs_2SiC.

TABLE 7
Valence Electron Counts for One Formula Unit of $PrOs_2SiC$, $ThOs_2SiC$, and $TbRe_2SiC$[a]

$Pr^{+3}(Os^{+2.5})_2Si^{-4}C^{-4}$ i.e., up to 5.5 e/Os may be involved in Os–Os bonding					
(A) C^{-4}	$(-2e-Os)_2$	4e	(B) C^{-4}:	$(-4e-Os)_2$	8e
	2 lone pairs on C	4e			
		8e			
Si^{-4}	$(-4e/3-Os)_6$	8e	Si^{-4}	$(-4e/3-Os)_6$	8e
$Os^{+2.5}$	$(-2e-C)_1$	2e	$Os^{+2.5}$	$(-4e-C)_1$	4e
	$(-4e/3-Si)_3$	4e		$(-4e/3-Si)_3$	4e
	$(-(5.5e/3)\cdot 2-Os)_3$	11e		$(-(5.5e/3)\cdot 2-Os)_3$	11e
		17e			19e
$Th^{+4}(Os^{+2})_2Si^{-4}C^{-4}$ i.e., 6 e/Os may be involved in Os–Os bonding or nonbonding on Os					
A) C^{-4}	$(-2e-Os)_2$	4e	(B) C^{-4}	$(-4e-Os)_2$	8e
	2 lone pairs on C	4e			
		8e			
Si^{-4}	$(-4e/3-Os)_6$	8e	Si^{-4}	$(-4e/3-Os)_6$	8e
Os^{+2}	$(-2e-C)_1$	2e	Os^{+2}	$(-4e-C)_1$	4e
	$(-4e/3-Si)_3$	4e		$(-4e/3-Si)_3$	4e
	$(-(6e/3)\cdot 2-Os)_3$	12e		$(-(4e/3)\cdot 2-Os)_3$	8e
		18e		one lone pair on Os	2e
					18e
$Tb^{+3}(Re^{+2.5})_2Si^{-4}C^{-4}$ i.e., 4.5 e/Re may be involved in Re–Re bonding					
C^{-4}	$(-4e-Re)_2$	8e			
Si^{-4}	$(-4e/3-Re)_6$	8e			
$Re^{+2.5}$	$(-4e-C)_1$	4e			
	$(-4e/3-Si)_3$	4e			
	$(-(4.5e/3)\cdot 2-Re)_3$	9e			
		17e			

[a] The superscripts in the formulas correspond to oxidation numbers (formal charges). The shared valence electrons are counted at both bonded atoms. In choosing among the possible valence electron distributions, it was assumed that the carbon and silicon atoms follow the 8-electron rule, and for the transition metal atoms we aimed for an electron count of 18.

A similar analysis of the bonding electrons can be made for $ThOs_2SiC$, as is demonstrated in detail in Table 7. In this compound, more valence electrons are available, and, in aiming for the inert gas shell number 18 for osmium, we have to assume nonbonding electrons at the carbon atoms (left-hand side) or at the osmium atoms (right-hand side of Table 7). By contrast, such an analysis can at most ascribe 17 electrons to each rhenium atom in $TbRe_2SiC$ (Table 7). Hence, this compound is electron deficient; i.e., not all bonding parts of the band structure can be used.

We have repeatedly shown that the transition elements in the structures of ternary transition metal carbides have an atomic environment which is compatible with the 18-electron rule, e.g., in Pr_2ReC_2 (17), $Ca_4Ni_3C_5$ (18), $Th_4Ni_3C_6$ (19), $Sc_5Re_2C_7$ (20), $Gd_3Mn_2C_6$ (21), $Yb_4Ni_2C_5$ (22), Er_2MnC_4 (23), $La_{12}Re_5C_{15}$ (24), $Tm_2Fe_2Si_2C$ (25), $GdRuC_2$ (26), and $Th_2Re_2Si_2C$ (27), while in others like YCoC (28, 29) and $La_5Os_3C_4$ (30) the transition element cannot reach the magic number of 18 electrons as is also demonstrated here for $TbRe_2SiC$. A review emphasizing the similarity of the transition metal carbon polyanion of these carbides with organometallic compounds has been published recently (31). These considerations of chemical bonding, which aim for conceptional simplicity, are rather crude. The real situation is certainly more complicated, as is demonstrated by the homogeneity range of $ThOs_{2+x}Si_{1-x}C$ and the two structure refinements resulting in the compositions $ThOs_{2.040(2)}Si_{0.960(2)}C$ and $ThOs_{2.284(2)}Si_{0.716(2)}C$.

ACKNOWLEDGMENTS

We thank Dipl.-Ing. U. Ch. Rodewald for the collection of the single-crystal diffractometer data, Dipl.-Chem. G. Kotzyba for the magnetic susceptibility measurements, and Mr. K. Wagner for investigating our samples with the scanning electron microscope. We are grateful to Dr. G. Höfer (Heraeus Quarzschmelze) and Dr. W. Gerhartz (Degussa AG) for generous gifts of silica tubes and osmium powder. This work was also supported by the Deutsche Forschungsgemeinschaft and the Fonds der Chemischen Industrie.

REFERENCES

1. L. Paccard, D. Paccard, and Ch. Bertrand, *J. Less-Common Met.* **135,** L5 (1987).
2. A. M. Witte and W. Jeitschko, *J. Solid State Chem.* **112,** 232 (1994).
3. Th. Hüfken, A.M. Witte, and W. Jeitschko, *Z. Kristallogr. Suppl.* **12,** 128 (1997).
4. K. Yvon, W. Jeitschko, and E. Parthé, *J. Appl. Crystallogr.* **10,** 73 (1977).
5. B. A. Frenz and Associates, Inc. and Enraf Nonius, 1986.
6. W. Jeitschko, "MTP International Review of Science" (D. W. A. Sharp, Ed.), Series Two, Vol. 5, Part 1, pp. 219–281. Butterworth, London, 1974.
7. A. M. Witte, "Struktur und Eigenschaften ternärer und quaternärer Carbide der Seltenerdmetalle und Actinoide mit Haupt- und Nebengruppenelementen." Doktorarbeit, Universität Münster, 1995.
8. Th. Hüfken, "Präparation und Charakterisierung binärer und ternärer Carbide sowie quaternärer Silicid-Carbide der Seltenerdmetalle mit Übergangsmetallen." Doktorarbeit, Universität Münster, 1997.
9. J. Rodriguez-Carvajal, FULLPROF version 2.6.1. Oct. 94, ILL (unpublished), based on the original code provided by D. B. Wiles and A. Sakthivel, *J. Appl. Crystallogr.* **14,** 149 (1981).
10. J. W. Visser, *J. Appl. Crystallogr.* **2,** 89 (1969).
11. H. Boller and H. Nowotny, *Monatsh. Chem.* **98,** 2127 (1967).
12. H. Boller and H. Nowotny, *Monatsh. Chem.* **99,** 721 (1968).
13. H. Boller, *Monatsh. Chem.* **102,** 431 (1971).
14. J. C. Schuster, *Z. Kristallogr.* **175,** 211 (1986).
15. R. Julien, N. Rodier, and V. Tien, *Acta Crystallogr. B* **34,** 2612 (1978).
16. M. H. Gerdes, W. Jeitschko, K. H. Wachtmann, and M. E. Danebrock, *J. Mater. Chem.* **7,** 2427 (1997).
17. W. Jeitschko, G. Block, G. E. Kahnert, and R.K. Behrens, *J. Solid State Chem.* **89,** 191 (1990).
18. U. E. Musanke and W. Jeitschko, *Z. Naturforsch.* **46b,** 1177 (1991).
19. M. A. Moss and W. Jeitschko, *Z. Metallkd.* **82,** 669 (1991).
20. R. Pöttgen and W. Jeitschko, *Z. Naturforsch.* **47b,** 358 (1992).
21. G. E. Kahnert and W. Jeitschko, *Z. Anorg. Allg. Chem.* **619,** 93 (1993).
22. U. E. Musanke, W. Jeitschko, and M. E. Danebrock, *Z. Anorg. Allg. Chem.* **619,** 321 (1993).
23. G. E. Kahnert, W. Jeitschko, and G. Block, *Z. Anorg. Allg. Chem.* **619,** 442 (1993).
24. R. Pöttgen, G. Block, W. Jeitschko, and R.K. Behrens, *Z. Naturforsch.* **49b,** 1081 (1994).
25. R. Pöttgen, Th. Ebel, C. B. H. Evers, and W. Jeitschko, *J. Solid State Chem.* **114,** 66 (1995).
26. R.-D. Hoffmann, K. H. Wachtmann, Th. Ebel, and W. Jeitschko, *J. Solid State Chem.* **118,** 158 (1995).
27. Th. Hüfken, A. M. Witte, and W. Jeitschko, *J. Alloys Compd.* **266,** 158 (1998).
28. M. H. Gerss and W. Jeitschko, *Z. Naturforsch.* **41b,** 946 (1986).
29. R. Hoffmann, J. Li, and R. A. Wheeler, *J. Am. Chem. Soc.* **109,** 6600 (1987).
30. K. H. Wachtmann, Th. Hüfken, and W. Jeitschko, *J. Solid State Chem.* **131,** 49 (1997).
31. R. B. King, *J. Organomet. Chem.* **536** and **537,** 7 (1997).